2009

A correlation between transport current density and grain connectivity in MgB2/Fe wire made from ball-milled boron

X Xu
University of Wollongong, xun@uow.edu.au

J H. Kim
University of Wollongong, jhk@uow.edu.au

S X. Dou
University of Wollongong, shi@uow.edu.au

S Choi
Magnet Dev Group - NIMS

J H. Lee
Korea university of Technology & Education

See next page for additional authors

A correlation between transport current density and grain connectivity in MgB2/Fe wire made from ball-milled boron

X. Xu, J. H. Kim, S. X. Dou, S. Choi, J. H. Lee et al.

Citation: J. Appl. Phys. **105**, 103913 (2009); doi: 10.1063/1.3129314
View online: http://dx.doi.org/10.1063/1.3129314
View Table of Contents: http://jap.aip.org/resource/1/JAPIAU/v105/i10
Published by the American Institute of Physics.

A correlation between transport current density and grain connectivity in MgB_2/Fe wire made from ball-milled boron

X. Xu,[1] J. H. Kim,[1,a)] S. X. Dou,[1] S. Choi,[2] J. H. Lee,[3] H. W. Park,[3] M. Rindfleish,[4] and M. Tomsic[4]

[1]*Institute for Superconducting and Electronic Materials, University of Wollongong, Wollongong, New South Wales 2522, Australia*

[2]*Magnet Development Group, Superconducting Materials Center, National Institute for Materials Science, 3-13 Sakura, Tsukuba, Ibaraki 305-0003, Japan*

[3]*Department of Materials Engineering, Korea University of Technology and Education, Cheonan, Chungnam 330-708, Republic of Korea*

[4]*Hyper Tech Research, Inc., 1275 Kinnear Road, Columbus, Ohio 43212, USA*

(Received 22 January 2009; accepted 6 April 2009; published online 27 May 2009)

Studies of the magnetic field dependence of the transport critical current density (J_{ct}) and the grain connectivity of MgB_2/Fe wires fabricated from ball-milled boron have been conducted in detail, and strong correlations have been found, as evidenced by differences in grain size, critical transition temperature, and resistivity. It was observed that the samples fabricated by ball milling had relatively small grain sizes, resulting in a strong field dependence of the J_{ct} in the high field region. On the other hand, the ball-milled boron was associated with poor connectivity between adjacent grains. It is clearly shown that the observed reduction in low field J_{ct} is related to the reduction in the superconducting area fraction (A_F) that is reflected by the connectivity factor. Even if high temperature sintering in all the samples can compensate for the degradation of the J_{ct} in the low field region, the subsequent grain growth is mainly responsible for the degradation of J_{ct} in the high field region. © *2009 American Institute of Physics*. [DOI: 10.1063/1.3129314]

I. INTRODUCTION

Enormous research efforts into areas such as materials performance properties, wire conductor development, and magnet demonstrations have been going on in the MgB_2 field since its discovery in 2001.[1] It is well known that the critical current density (J_c) of pure MgB_2 is drastically decreased with an increasing external magnetic field because of its poor flux pinning properties, when compared to high temperature superconductors. Quite interestingly, however, unique features of the superconductivity observed in the MgB_2 are related to its two-band nature and the lack of weak links at the grain boundaries.[2] In addition, the advantages of the simple binary composition, the transition temperature of 39 K, and the low cost of the starting materials have been sufficient to put it on the road to real applications.

So far, our group has achieved improvements in the critical current density (J_c) and upper critical field (B_{c2}) through ball-milling processing. As the first step, the effects of ball milling pure boron (B) powder (99%, amorphous) using different media, such as acetone, ethanol, and toluene, were studied. Using toluene led to enhancements in the magnetic critical current density (J_{cm}) in high field.[3] For the second step, we prepared samples from low grade boron (96%) with semicrystalline phase via ball milling in toluene as well. The results of this have demonstrated the possibility and cost effectiveness of fabricating high performance samples using low grade boron.[4] All previous reports in the literature have been directed toward finding effective means of reducing the strong field dependence under high field. However, the low field performance might be further improved to attain a particular level, for example, $>10^6$ A cm^{-2}. It is well known that the critical current density in self-field decreases due to the degradation of the connectivity between grains.[5] In particular, the initial magnesium (Mg) and B powders that we previously studied in pellet form are loosely connected before the reaction. After heat-treatment, even if reacted MgB_2 is expected to be more consolidated, it is likely to have some porosity, depending on the packing conditions in *in situ* processing.[6,7] Therefore, it would be hard to estimate the connectivity factor from those pellet samples. What is important is that the results on our bulk samples still gave us the possibility that low grade 96% B powder can be adopted for industrial applications.

For conductors, the powder-in-tube (PIT) method is very common, in which a metallic sheath is packed with powders and then is drawn. In the wire conductor, the relative amount of porosity is decreased due to mechanical deformation, which results in improved core densification, unlike what is seen in pellet samples. Therefore, we need to evaluate the correlation between the transport current density and the grain connectivity in wire conductor. In addition, there are some more detailed reasons for this study. The transport critical current density (J_{ct}) is the real useful J_c that flows through the whole of the sample, while the magnetic critical current density (J_{cm}) overestimates the real J_c at low fields and underestimates it at high fields.[8] This difference between J_{cm} and J_{ct} in MgB_2 is related to the microstructure of the superconducting MgB_2 core. There are superconducting screening currents flowing on different length scales due to sample porosity and agglomeration of superconducting

a)Author to whom correspondence should be addressed. Electronic mail: jhk@uow.edu.au.

crystals.[9] Some simulations show that major defects in the superconducting core will have an affect on the transport current.[10]

In the present work, therefore, studies of the transport critical current density (J_{ct}) and grain connectivity of the MgB_2/Fe wires fabricated from ball-milled boron have been conducted in detail, and strong correlations have been found. We evaluated the superconducting properties of MgB_2/Fe made from low-grade 96% commercial boron powder with a strong crystalline phase. The particle size of the boron, the transport and the magnetic critical current densities (J_{ct} and J_{cm}), the critical temperature (T_c), the residual resistivity ratio (RRR), the upper critical field (B_{c2}), the irreversibility field (B_{irr}), and the microstructures of MgB_2 made from ball-milled boron are presented in comparison with reference samples made at different sintering temperatures.

II. EXPERIMENTAL METHODS

MgB_2/Fe monofilament wires were prepared by an *in situ* reaction process and the PIT method. Boron powder (96% purity, ~0.65 μm, crystalline, Tangshan WeiHao, China) and that was processed by ball milling, with toluene as the ball-milling medium. The ball-milling process was carried out for 12 h at a rotation speed of 160 rpm. The powder to ball ratio was 1: 16 in a planetary ball mill with an agate jar and balls 5 mm and 10 mm in size. The powders were then dried in a vacuum oven to evaporate the toluene. For our experiments, two kinds of boron powder were prepared, with and without ball milling: these are denoted by BP96 and P96, respectively. Here, the ball-milled boron is denoted by the initial B.

Magnesium (99%, 325 mesh), and the different boron powders with the nominal atomic ratio of Mg:B=1:2 were mixed through grinding and were put into Fe tubes with a length of 140 mm, an outer diameter of 10 mm, and an inner diameter of 8 mm. The packing process was carried out in air. Both ends of the tubes were sealed with aluminum pieces, and then the tubes were drawn to a wire with a diameter of 1.4 mm. Short wire samples (4 cm each) were sealed with Zr foil, then sintered with a heating rate of 5 °C min^{-1} in flowing high purity Ar to 650–800 °C and held at the final temperature for 30 min, followed by a furnace cooling to room temperature. The volume fraction of the superconducting core in the final wire was approximately 48%.

The boron powder particle size and distribution were determined by a JL-1166 Laser Particle Sizer (Chengdu, China) from Tangshan WeiHao. The phase and crystal structure of all the samples were investigated by x-ray diffraction (XRD). The crystal structure was refined with the aid of the program Jade (ver. 5.0). The grain morphology and the microstructure of the MgB_2 were studied by scanning electron microscopy (SEM). The transport current (I_c) at 4.2 K was measured by the standard dc four-probe resistive method with a criterion of 1 μV cm^{-1} in magnetic fields up to 12 T. The magnetic J_c (J_{cm}) was derived from the width of the magnetization loop using the extended Bean's model. T_c was determined using the standard ac four-probe method. In addition, $B_{c2}(T)$ and $B_{irr}(T)$ were defined as the fields where the temperature dependent resistance at constant magnetic field $R(B_{c2},T)=0.9R_{ns}$ and $R(B_{irr},T)=0.1R_{ns}$, respectively, with R_{ns} being the normal state resistance near 40 K.

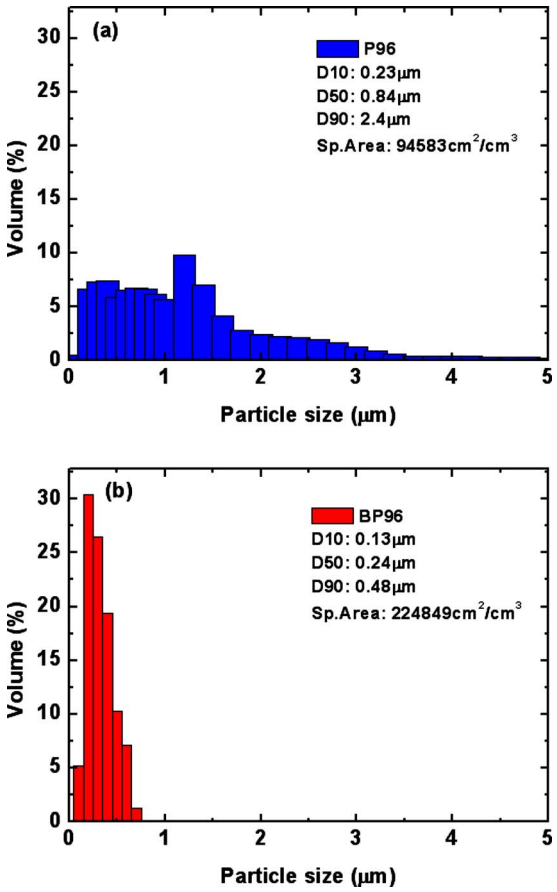

FIG. 1. (Color online) Particle size distributions for (a) as-supplied (P96) and (b) ball-milled boron (BP96) powders.

III. RESULTS AND DISCUSSION

Figure 1 shows the particle size distributions of (a) the as-supplied boron, P96, and (b) the ball-milled boron powder, BP96. It can be clearly seen that the average particle size of the original boron powder, P96, became smaller after ball milling. For example, the median value (D50) decreased from 0.84 to 0.24 μm. The size distribution of the BP96 also became narrow. If we neglect the effect of the powder shape, the small particle size led to a more than twofold increase in the specific surface area, which may tend to improve the reactivity between the powders, even under the same solid reaction conditions. It is well known that the grain size of the MgB_2 as it is formed depends on the particle size of the boron powder.[11,12] The small grains could act as strong flux pinning centers for MgB_2. Therefore, it is not surprising that the MgB_2 prepared from the ball-milled boron powder (BP96) had small grain size and showed improved superconducting properties, especially high field performance.

These can be further supported by microstructure observation. SEM images of MgB_2 wires made from (a) as-supplied boron (P96) and (b) ball-milled boron powders (BP96), denoted as WPS700 and WBPS700, respectively, are

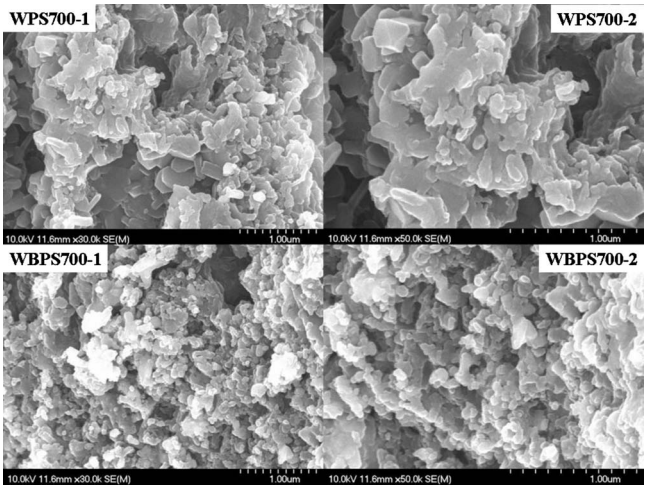

FIG. 2. SEM images at two magnifications for (top) wire sample prepared from as-supplied boron, and (bottom) wire sample prepared from ball-milled boron. All samples were sintered at 700 °C for 30 min.

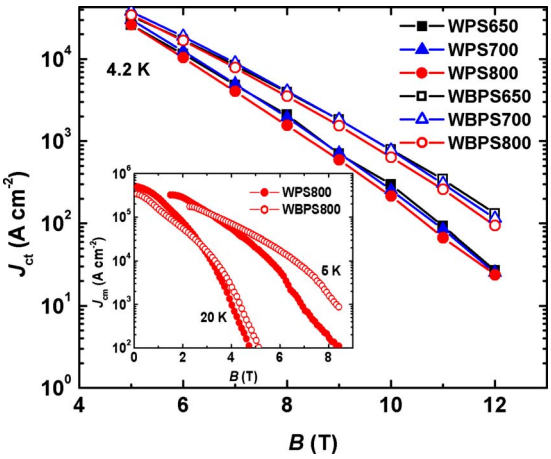

FIG. 3. (Color online) Transport critical current density (J_{ct}) for all MgB_2 wires as a function of external magnetic field at 4.2 K. The inset shows the field dependences of the magnetic critical current density (J_{cm}) at 5 K and 20 K with WPS800 and WBPS800.

shown in Fig. 2, with all samples sintered at 700 °C for 30 min. Here, the wire samples are identified by the initial W, and the sintering temperature is denoted by the numerals. It is clearly observed that the average grain size of the sample prepared from the ball-milled boron is much smaller than in the sample made from the as-supplied boron. It also seems to be more consolidated. From the crystallinity point of view, on the other hand, the sample prepared from the ball-milled boron showed poor crystallinity, as evidenced by the degradation of the transition temperature, to be discussed below. The crystallinity effect has already been reported in our previous work.[4] Better J_c properties observed in samples that were heated at low temperatures and exhibit broad XRD peaks, in particular, (110) peak of MgB_2, it is believed to be due to smaller grown grains with poor crystallinity, which increase pinning strength at the grain boundaries.[13] In general, the crystallinity, as reflected by the lattice parameters, secondary phases, and microstrain, is an important factor determining the T_c. We also observed that the MgO fraction increased over the entire MgB_2 volume after ball milling, as evidenced by XRD measurements. The increased MgO may have caused loss of the initial stoichiometry, which affects the level of induced strain due to Mg deficiency. As the main secondary phase, we cannot neglect MgO in the matrix, although the MgO particles cannot be directly distinguished from the SEM images. Among our samples, the ball-milled samples (WBPS700) had a higher MgO intensity increase, approximately 9%, compare to samples (WPS700) prepared from as-supplied boron. Due to the large fraction of MgO, therefore, they showed increased $\Delta\rho$ ($\rho_{300\ K}-\rho_{40\ K}$) and decreased RRR ($\rho_{300\ K}/\rho_{40\ K}$) values (as shown in Table I), a degraded grain connectivity factor (A_F), and reduced transport critical current density (J_{ct}), which offset the strong pinning properties due to the effect of small grain size.

A comprehensive study comparing the positive "*small grain size*" and negative "*weak connectivity*" effects on the J_{ct} was conducted. The $J_{ct}-B$ performance of the two kinds of the samples sintered at temperatures from 650 to 800 °C, denoted by WPS650, WPS700, WPS800, WBPS650, WBPS700, and WBPS800, respectively, is shown in Fig. 3. It can be clearly seen that J_{ct} of samples prepared from the ball-milled boron showed better performance in the field range of 5–12 T. This indicates that ball milling causes reduction in the MgB_2 grain size, which could act as a source of strong pinning centers due to the increased number of grain boundaries, as mentioned above. However it was concluded that the ball milling could not help to improve the J_{ct} at magnetic fields below 5 T. The inset shows the field dependences of the magnetic critical current density (J_{cm}) at 5 K and 20 K for WPS800 and WBPS800. Compared to the magnetic J_{cm} under magnetic fields of 5–8 T, the transport J_{ct} increment is lower from Fig. 4, because the transport current capacity is the real useful J_c that flows through the whole of the sample. That is to say, the difference between J_{cm} and J_{ct} in MgB_2 may be related to features of the microstructure of the superconducting MgB_2 core, such as porosity, agglom-

TABLE I. The measured resistivity (ρ) values, RRR, active cross-sectional area fractions (A_F), critical temperatures (T_c), and lattice strain for MgB_2 wire made from ball-milled boron and from as-supplied boron under comparable sintering conditions.

Samples ID	$\rho_{40\ K}$ ($\mu\Omega$ cm)	$\rho_{300\ K}$ ($\mu\Omega$ cm)	$\Delta\rho$ ($\rho_{300\ K}-\rho_{40\ K}$) ($\mu\Omega$ cm)	RRR	A_F	T_c (K)	lattice strain (%)
WPS650	34.8	78.7	43.9	2.26	0.166	37.9	0.273(1)
WPS800	20.3	49.4	29.1	2.43	0.250	38.1	0.284(1)
WBPS650	84.5	151.1	66.6	1.78	0.109	37.4	0.338(1)
WBPS800	64.3	125.2	60.9	1.94	0.119	37.4	0.315(1)

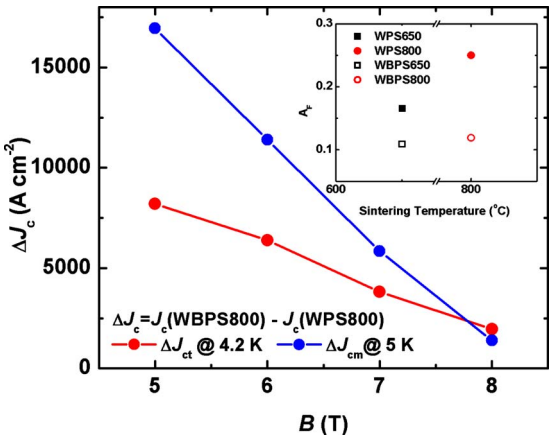

FIG. 4. (Color online) Compared to the increment of magnetic critical current density (J_{cm}) at 5 K and transport critical current density (J_{ct}) at 4.2 K under magnetic fields of 5–8 T with WPS800 and WBPS800. The inset shows the calculated active cross-sectional area fraction (A_F) represents the connectivity factor with WPS650, WPS800, WBPS650, and WBPS800.

eration of superconducting crystals, and fraction of MgO as the main secondary phase. These could have negative effects on the J_{ct}, by acting as obstacles to current flow. Quite interestingly, the effects of these obstacles do not appear in magnetic loop measurements. That is why the magnetic J_{cm} does not represent the real J_c of MgB_2 wires.[8]

According to the Rowell connectivity analysis, the calculated active cross-sectional area fraction (A_F) represents the connectivity factor between adjacent grains.[14,15] From the inset of Fig. 4 shows, the A_F for all samples increased as the sintering temperature increased. This indicates that additional grain growth occurs due to high temperature sintering. The larger grains are also accompanied by improved density and grain connectivity. Thus the A_F increases. Yamamoto and co-workers[5,6] found the critical current density is approximately proportional to the electrical connectivity, the elementary pinning force of grain boundaries, and the reciprocal grain size. So, the connectivity between the grains of the ball-milling samples should be further improved for industrial applications.

This can be further supported by the RRR ($\rho_{300\ K}/\rho_{40\ K}$) values from Table I. The RRR values for all samples were decreased through low temperature sintering, as well as by ball milling. A large RRR is an important determinant of a high quality sample. In particular, an increased $\rho_{40\ K}$ value is due to increased impurity scattering in the lattice. That is to say, it causes an increase in the lattice strain, resulting in degradation of the transition temperature.

If disorder is an important factor affecting the transition temperature of MgB_2 samples, there should be a relation between the resistivity and the transition temperature. In a previous review, the Testardi correlation, an empirical relation between the RRR and the transition temperature, was discussed in connection with Nb–Ge film.[16] As shown in Fig. 5(a), we found that the critical temperature shows a dependence on the RRR, which can be expressed by a simple linear function. A more interesting correlation is suggested in a recent review of Eisterer between the transition temperature and the normalized resistivity,[17] the ratio of the residual

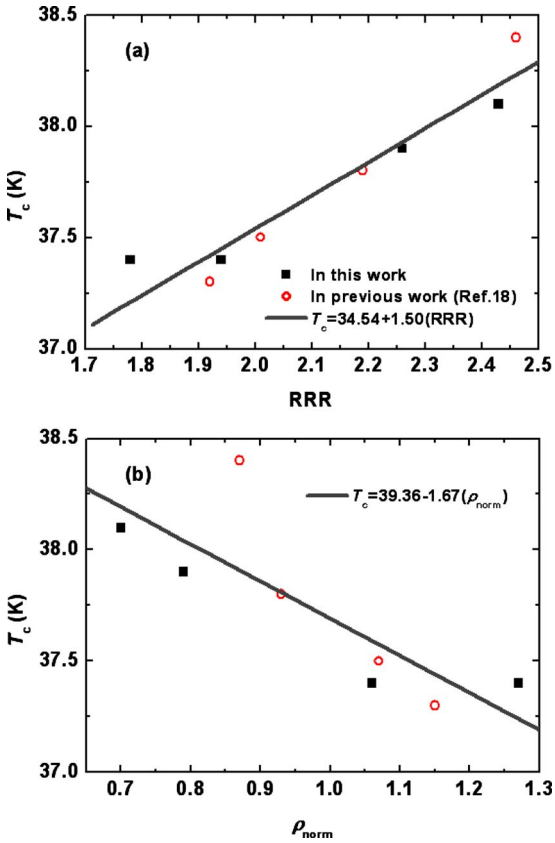

FIG. 5. (Color online) The correlations between (a) the critical temperature (T_c) and the RRR, and (b) the T_c and the normalized resistivity (ρ_{norm}).

resistivity to the difference in resistivity between 300 and 40 K, $\rho_{norm}=\rho_{40\ K}/\Delta\rho$, where $\Delta\rho=\rho_{300\ K}-\rho_{40\ K}$. Various reported data were compared, and it was argued that the transition temperature can be described by a simple linear relation, $T_c=(39.43-2.515\ \rho_{norm})$ K. We found that our data are also compatible with a similar linear relation: $T_c=(39.36-1.67\ \rho_{norm})$ K, as shown in Fig. 5(b).[18] Thus, degradation of the transition temperature is strong evidence of poor crystallinity and connectivity.

From the resistance (R)-temperature (T) curves, the temperature dependence of B_{c2} and B_{irr} for all the samples is shown in Fig. 6. As can be seen in the Figure, the values of B_{c2} and B_{irr} were enhanced via ball milling as well as by low temperature sintering. The B_{irr} showed the same trends as

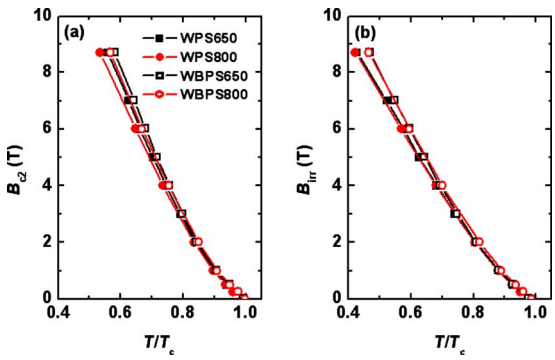

FIG. 6. (Color online) Temperature dependence of (a) the upper critical field (B_{c2}) and (b) the irreversibility field B_{irr} for MgB_2 wires as a function of sintering temperature and ball-milling condition.

$J_{ct}(B)$ at 4.2 K, that is, a significant increase in the upper critical field, B_{c2}, is the main cause of the enhancement of the critical current density, J_c, in the high field region. Also, the $B_{c2}-T$ curves of the samples show that a low sintering temperature is better than a high one, which indicates that more defects or poor crystallinity within grains induces lattice strain, decreases T_c, and increases B_{c2}.

IV. CONCLUSIONS

In summary, a comprehensive study of ball-milling effects on the transport critical current density (J_{ct}) and grain connectivity factor (A_F) of MgB_2/Fe wires has been conducted. We observed that lattice disorder increased due to the ball milling. It caused both a slight reduction in the transition temperature and degradation of connectivity. The reduction in the transition temperature can change the upper critical field, so that the upper critical field is mostly affected by the lattice disorder. A significant increase in the upper critical field is the main cause for the enhancement of the critical current in the high field region. On the other hand, high temperature sintering in all types of samples can improve J_{ct} in the low field region because it leads to good grain connectivity.

ACKNOWLEDGMENTS

The author would like to thank Dr. T. Silver for her helpful discussions and Dr. J. Horvat for his help with measurements at the Institute for Superconducting and Electronic Materials, University of Wollongong. This work was supported by the Australian Research Council, Hyper Tech Research, Inc., OH, USA, Alphatech International Ltd., NZ, TangShan Weihao Magnesium Powder Co., Ltd., China, and the University of Wollongong.

[1] J. Nagamatsu, N. Nakagawa, T. Muranaka, Y. Zenitani, and J. Akimitsu, Nature (London) **410**, 63 (2001).
[2] D. C. Larbalestier, M. O. Rikel, L. D. Cooley, A. A. Polyanskii, J. Y. Jiang, S. Patnaik, X. Y. Cai, D. M. Feldmann, A. Gurevich, A. A. Squitieri, M. T. Naus, C. B. Eom, E. E. Hellstrom, R. J. Cava, K. A. Regan, N. Rogado, M. A. Hayward, T. He, J. S. Slusky, P. Khalifah, K. Inumaru, and M. Haas, Nature (London) **410**, 186 (2001).
[3] X. Xu, J. H. Kim, W. K. Yeoh, Y. Zhang, and S. X. Dou, Supercond. Sci. Technol. **19**, L47 (2006).
[4] X. Xu, J. H. Kim, M. S. A. Hossain, J. S. Park, Y. Zhao, S. X. Dou, W. K. Yeoh, M. Rindfleisch, and M. Tomsic, J. Appl. Phys. **103**, 023912 (2008).
[5] A. Yamamoto, J. Shimoyama, K. Kishio, and T. Matsushita, Supercond. Sci. Technol. **20**, 658 (2007).
[6] T. Matsushita, M. Kiuchi, A. Yamamoto, J. Shimoyama, and K. Kishio, Supercond. Sci. Technol. **21**, 015008 (2008).
[7] J. H. Kim, M. Maeda, Y. Zhao, D. Q. Shi, S. X. Dou, S. Choi, and T. Kiyoshi, Physica C **468**, 1813 (2008).
[8] J. Horvat, W. K. Yeoh, J. H. Kim, and S. X. Dou, Supercond. Sci. Technol. **21**, 065003 (2008).
[9] J. Horvat, S. Soltanian, X. L. Wang, and S. X. Dou, Appl. Phys. Lett. **84**, 3109 (2004).
[10] E. Bartolome, F. Gömöry, X. Granados, T. Puig, and X. Obradors, Supercond. Sci. Technol. **18**, 388 (2005).
[11] S. K. Chen, K. A. Yates, M. G. Blamire, and J. L. MacManus-Driscoll, Supercond. Sci. Technol. **18**, 1473 (2005).
[12] W. Häßler, B. Birajdar, W. Gruner, M. Herrmann, O. Perner, C. Rodig, M. Schubert, B. Holzapfel, O. Eibl, and L. Schultz, Supercond. Sci. Technol. **19**, 512 (2006).
[13] A. Yamamoto, J. Shimoyama, S. Ueda, Y. Katsura, I. Iwayama, S. Horii, and K. Kishio, Appl. Phys. Lett. **86**, 212502 (2005).
[14] J. M. Rowell, Supercond. Sci. Technol. **16**, R17 (2003).
[15] J. Jiang, B. J. Senkowicz, D. C. Larbalestier, and E. E. Hellstrom, Supercond. Sci. Technol. **19**, L33 (2006).
[16] L. R. Testardi, R. L. Meek, J. M. Poate, W. A. Royer, A. R. Storm, and J. H. Wernick, Phys. Rev. B **11**, 4304 (1975).
[17] M. Eisterer, Supercond. Sci. Technol. **20**, R47 (2007).
[18] J. H. Kim, S. X. Dou, J. L. Wang, D. Q. Shi, X. Xu, M. S. A. Hossain, W. K. Yeoh, S. Choi, and T. Kiyoshi, Supercond. Sci. Technol. **20**, 448 (2007).